Organo-polyoxometalate-Based Hydrogen-Bond Catalysis

Debora Vilona, Moreno Lelli, Elise Dumont, Emmanuel Lacôte

Organo-polyoxometalate-Based Hydrogen-Bond Catalysis

Debora Vilona,[a,b,c] Moreno Lelli,*,[b,d] Elise Dumont,*,[c] Emmanuel Lacôte*,[a]

Dedication ((optional))

Abstract: Several urea-inserted organo-polyoxometalates (POMs) derived from polyoxotungstovanadate $[P_2V_3W_{15}O_{61}]^{9-}$ were prepared. The insertion of the carbonyl into the polyoxometallic framework activates the urea toward Hydrogen-bond catalysis. This was shown on the Friedel-Crafts arylation of *trans*-β-nitrostyrene. Modelling shows that the most stable form of the organo-POMs features an anti-parallel arrangement of the two N–H bonds, but that the likely catalytically active parallel form is accessible at room temperature. Finally, it is possible that the oxo substituents next to the vanadium atoms may help the approach of the nucleophile via H-bonding.

Polyoxometalates (POMs) have been extensively used as acid catalyst since the 1970s, both under homogeneous and heterogeneous conditions.[1–5] Fully protonated POMs are called heteropolyacids. Some approach the superacidic behavior, and they have been fruitfully used in industry.[6–9] However, there are only a limited number of heteropolyacids used in catalysis because the acidity derives exclusively from the inorganic structure, and there are not that many POM frameworks stable enough at acidic pH, and/or where the proton/oxide interaction can be harnessed for reactivity. Besides, heteropolyacids are often not soluble in organic solvents, precluding any use under homogeneous conditions. Some of these limitations can be solved upon introducing appropriate counterions,[10,11] although that carries the risk that the polyanion becomes just a weakly coordinating spectator ion.[12]

Organo-POMs, which combine the properties of the inorganic scaffolds and of the covalently-bound organic moieties,[13,14] offer a new handle for diversity in POM-based catalysis.[5,15–20] For example, we showed how the unique insertion[21–25] of diolamides into the structure of polyoxotungstovanadate $[P_2V_3W_{15}O_{61}]^{9-}$ enhanced the acidity of the amide proton,[26] generating the first truly hybrid heteropolyacid.[25] The catalytic activity stemmed from the facilitated transfer of the activated proton to substrates.

Nature also achieves acid-catalysis by relying on strategically positioned H-bonds, which cumulatively act like a proton, but where no proton is actually transferred to the substrate. This has led to a huge body of work in organocatalysis, but has not been examined at all in POM chemistry. We report herein how our carbonyl-insertion strategy can be directed toward H-bond catalysis.

We approached the problem through ureas, which are known to catalyze many organic reactions by hydrogen-bonding activation.[27,28] In 2011, Oble et al. had shown that also ureas could be inserted into $[P_2V_3W_{15}O_{61}]^{9-}$, although the resulting hybrids were only examined for their oxidative properties.[22] We surmised that the withdrawing effect of the polyoxometallic framework at play with amides could potentially also activate the grafted urea toward H-bond catalysis.

Using the synthetic procedure previously developed in our group,[22] we prepared five urea-inserted organo-POMs (**1a-e**, Figure 1). The phenyl (**1a**), *p*-methoxy-phenyl (**1b**), and *p*-CF₃-phenyl (**1c**) derivatives were known. To have an array of electron-diverse potential catalysts we added 3,5-*bis*-trifluoromethyl-phenyl- (**1d**) and hexyl- (**1e**) substituted compounds. All reactions were essentially quantitative, the smaller variations being due to partial loss upon filtration of the solid POMs.
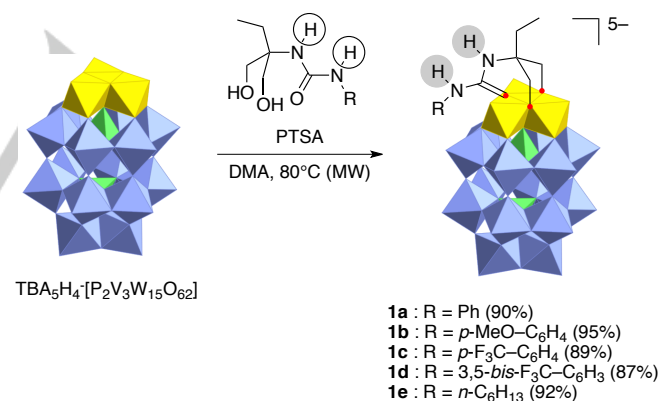

$TBA_5H_4^-[P_2V_3W_{15}O_{62}]$

1a : R = Ph (90%)
1b : R = *p*-MeO–C₆H₄ (95%)
1c : R = *p*-F₃C–C₆H₄ (89%)
1d : R = 3,5-*bis*-F₃C–C₆H₃ (87%)
1e : R = *n*-C₆H₁₃ (92%)

Figure 1. Preparation of the urea-POMs

[a] D. Vilona, Dr. E. Lacôte
     Univ Lyon, Université Claude Bernard Lyon 1, CNRS, CNES, ArianeGroup, LHCEP, Bât. Raulin, 2 rue Victor Grignard, F-69622 Villeurbanne, France; E-mail: emmanuel.lacote@univ-lyon1.fr
[b] D. Vilona, Prof. M. Lelli
     Univ Lyon, Université Claude Bernard Lyon 1, École Normale Supérieure de Lyon, CNRS, CRMN, 5 rue de la Doua 69100 Villeurbanne, France
[c] D. Vilona, Prof. E. Dumont
     Univ Lyon, ENS Lyon, Univ Claude Bernard Lyon 1, CNRS, LCENS, UMR 5182, ENS de Lyon, 46 allée d'Italie, F-69364 Lyon cedex 07, France; E-mail: elise.dumont@ens-lyon.fr
[d] Prof. M. Lelli
     Magnetic Resonance Center and Department of Chemistry, University of Florence, Italy; E-mail: moreno.lelli@unifi.it

     Supporting information for this article is given via a link at the end of the document.((Please delete this text if not appropriate))

The organo-POMs obtained were fully characterized. Of particular note is a strong downfield shift of the ¹H-NMR signals of the ureic protons when anchored to the vanadate crown (Table 1). The chemical shifts for the N–H protons closer to the diol terminus range from 5.29 ppm for the urea leading to **1e** to 5.76 ppm for that leading to **1d** when these ureas are not inserted into the POM. The signals are strongly deshielded in the POMs, from 7.18 ppm in alkyl substituted **1e**, to 9-10 ppm for the aryl-substituted **1a-d**. The chemical shifts of the "external" protons (those directly attached to the variable part of the ureas) exhibit a similar trend, albeit less marked. The chemical shifts range from 5.18 ppm

(hexyl) to 7-8 ppm in the free arylureas. They move downfield to 6.85 ppm in **1e** and to 8.5-9.5 ppm for **1a-d**.

Table 1. ^{1}H NMR chemical shifts of the ureic protons in the free ligands and in the respective grafted derivatives

POM	δ in free urea		δ in organo-POM	
	HN "diol-side"	HN–R	HN "internal"	HN–R
1a	5.43	7.38	9.64	8.63
1b	5.33	7.05	9.23	8.45
1c	5.67	7.86	9.79	8.80
1d	5.76	8.07	10.1	9.10
1e	5.29	5.18	7.18	6.85

A similar deshielding was observed in the signals associated to the amide protons in the amide-inserted polyoxovanadates (in the "internal" position). It was shown to be a sign of an increased acidity of the corresponding proton, so we considered the present observations as a good sign that the POM may also become a H-bond catalyst. The second good omen is that the chemical shifts variations appear correlated to the substituents on the initial urea (at least for the aryl derivatives), despite the presence of the additional nitrogen atom which could have offset the electronic effects. Here, a donating substituent (as in **1b**) leads to less deshielding than withdrawing ones (as in **1c-d**).

To understand better the system we sought help from modeling. The geometries of all hybrids were optimized relying on density functional theory, at the DFT-M06-2X/6-31+G(d,p)/LANL2DZ level of theory using the Gaussian16 suite of programs[29] (Figure 2 and Table S1).
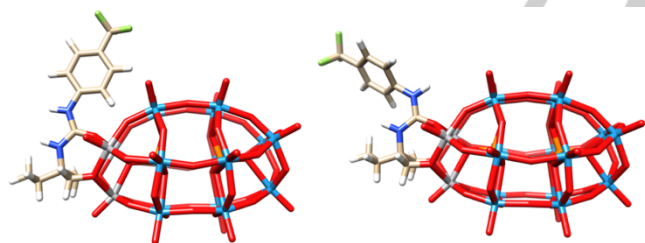

Figure 2. Calculated structures for parallel (left) and and antiparallel (right) conformations of urea@POM **1c** (DFT-M06-2X/6-31+G(d,p)/LANL2DZ level of theory).

The POM calculated structures shared common features. The most stable conformation has the N–H bonds not parallel (Figure 2, right). The "internal" N–H is indeed antiparallel to the vanadium-linked C=O bond, but the external one points toward the POM surface. The parallel position is taken by the urea substituent. This might reflect the increased acidity of the H atom, leading to the establishment of a favorable H-bond with the POM anionic surface, or it might be due to steric strain between said surface and the urea R-group in the classical parallel arrangement.

The parallel, catalytically active, conformers (e. g. left, Figure 2) lie 3-4.5 kcal.mol^{-1} higher than the anti-parallel ones (e. g. 3.7 kcal.mol^{-1} for **1c**, see Table S1). For **1a**, a transition state lining was located (qst3 keyword) at 8.9 kcal.mol^{-1}, meaning that

interconversion between both forms is possible – and presumably catalysis – at room temperature.

The bond lengths (Table S1) are constant, regardless of the substituents. That is true for both N–H bonds, the C=O, or the N–C bonds to the carbonyl carbon, as well as the N–C bond of the "internal" N to the quaternary carbon of the diol. The only exceptions are the N–C bond lengths of the "external" N to the R substituent, which are longer in **1e**, and shorter in **1a-d**, especially so with **1c-d**. This is likely because **1e** is an alkyl urea, therefore the bond is longer. Overall, our modeling indicates that the organo-POM system is quite rigid with some variation around one of the N–H bonds.

To test the potential catalytic properties of our organo-POMs, we focused on the Friedel-Crafts alkylation of indole with *trans*-β-nitrostyrene (TBNS) as benchmark reaction. This reaction is generally catalyzed by electron-poor substituted (thio)urea.[30] It proceeds via the activation of the vinyl group of the TBNS through hydrogen-bond interaction of the nitro with the urea protons of the catalyst. This induces the polarization of the bonds in the olefinic substrate which promotes the nucleophilic addition of the indole ring onto the β-carbon of the TBNS. In a typical experiment (Table 2, Entry 1), 1 equivalent of TBNS (0.4 mmol scale) was reacted with 1.5 equivalent of indole in the presence of 2 mol% of **1a** in warm (50°C) acetonitrile. The reaction was monitored by ^{1}H NMR.

Table 2. Probe of the H-bond catalysis with organo-POMs: Friedel-Crafts arylation of *trans*-β-nitrostyrene.

Entry[a]	Catalyst	TBNS conversion (%)[b]				Yield (%)
		24h	48h	72h	96h	
1	**1a**	7	25	44	66	-
2	**1b**	6	13	33	46	
3	**1c**	18	52	99		92
4	**1d**	16	54	98		
5	**1e**	-	14	37	48	
6	-	-	-	-	-	-
7	diolurea[c]	-	-	-	-	
8	TBA$_5$H$_4$ [P$_2$W$_{15}$V$_3$O$_{62}$]	9	21	35	41	
9	TBA$_9$ [P$_2$W$_{15}$V$_3$O$_{62}$]	-	-	-	-	
10	TBA$_5$H$_4$ POM[d] + p-F$_3$C-C$_6$H$_4$ urea	10	15	25	39	
11	**6**[e]				56	

[a] Reaction conditions: TBNS (0.4 mmol, 1 equiv.), Indole (0.6mmol, 1.5 equiv), catalyst (8 µmol, 2 mol%) dissolved in dry MeCN (1 mL) in Schlenk tube under argon at 50°C; [b] measured by ^{1}H NMR; [c] all diolureas were tested (see Table S2) in the SI; [d] POM = [P$_2$W$_{15}$V$_3$O$_{62}$]$^{9-}$; [e] 1 mol% of ^{6} was used.

Gratifyingly, the reaction proceeded, albeit slowly. Indole **2** was formed, and the reaction reached 66% conversion after 4 days, while the same urea not grafted to the POM led to no conversion (entry 7). When an electron-donating group was positioned on the urea, the reaction proceeded more slowly (entry 2). Conversely, electron-withdrawing substituents accelerated the addition, which was over (and essentially quantitative) in under three days (entries 3-4). This is compatible with a more activated H-bond catalyst, as expected.

We carried additional experiments to characterize more precisely the mechanism of the catalysis. First, the reaction studied is catalyzed by Brønsted acids, such as the parent $(TBA)_5H_4[P_2W_{15}V_3O_{62}]$, albeit at a reduced rate (entry 8). The POM structure itself is not catalytically active, once the protons around it have been removed (entry 9). Finally, mixtures of uncomplexed ureas and $(TBA)_5H_4[P_2W_{15}V_3O_{62}]$ behaved as $(TBA)_5H_4[P_2W_{15}V_3O_{62}]$ (entry 10).

Overall, that makes us certain that the reactions in entries 1-5 proceed via activation of the nitro group in the electrophile by H-bonding with the ureas, since there are no protons around POMs **1a-e**, and the Brønsted acid-catalyzed background reaction is much slower anyway. The POM framework likely polarizes the urea, which in turn activates the electrophile in the rate determining step. In order to further support this hypothesis, we carried out additional experiments.

First, we measured the formation constants of the nitro/urea pairs for POMs **1a-d** and their corresponding free ureas. In a typical procedure, a solution of urea in CD_3CN (1 eq) was titrated with a solution of TBNS in CD_3CN (by increments of 0.25 equiv. of TBNS to 2 equiv. of TBNS). The ^1H-NMR spectrum of the mixture was recorded after each addition.

With **1a** and **1b** (and their corresponding free ureas) no observable change was observed in the ^1H NMR signals (see Figure S2), suggesting that the interaction is at best too weak for the sensitivity of the technique. In contrast, the electron poor ureas and POMs **1c-d** led to observable shifts. Interestingly, the signals of the N–H protons are more affected by the presence of TBNS in the free ureas, rather than in the POMs. For example, the N–H signal at 5.67 ppm in p-F_3C–C_6H_4–N(H)–C(=O)–N(H)diol exhibits a ~10 Hz downfield shift upon addition of 1.5 equivalents of TBNS (Figure S3), whereas in **1c**, the N–H protons at 8.98 ppm only shifted downfield by about 3 Hz after the addition of 1.5 equivalents of TBNS. The signal of the other urea N–H proton at 7 ppm is too broad to be correctly exploited. That allowed us to calculate an association constant of 4.4 M^{-1} for p-F_3C–C_6H_4–N(H)–C(=O)–N(H)diol and 0.8 M^{-1} for **1c**. A similar trend was observed for the couple 3,5-bis-F_3C–(C_6H_3)–N(H)–C(=O)–N(H)diol / **1d**.
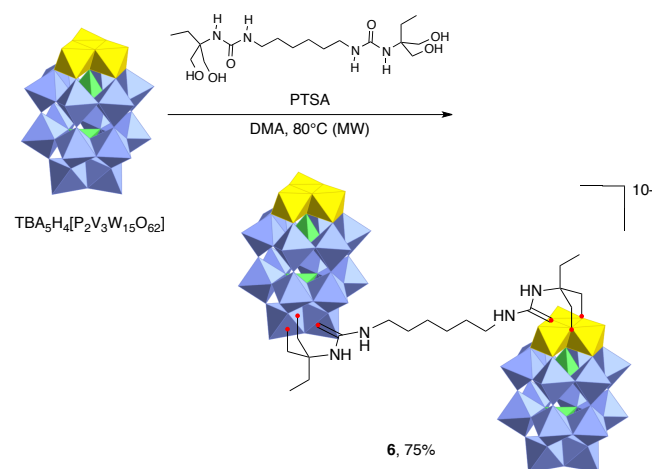
We next looked at the reaction of three more indoles (Figure 2). Methoxy-indole **3** reacted with a similar kinetic profile as **1**. In contrast, chloro-indole **4** reacted more slowly, reaching 94% conversion only after 4 days. Finally, N-methyl indole 5 was much less reactive, only reaching 63% conversion.

We believe the previous experiments confirm that the POM-urea acts as a H-bond organocatalyst. Indeed, the reaction does not proceed from a better association of the substrate to the POM, as the latter have lower association constants to the substrate (maybe due to steric hindrance that develops in the "urea" configuration between the urea substituent and the POM framework). Yet, the catalysis proceeds with the same features as urea-catalysis (electron-poor substrates are disfavored, electron-withdrawing substituents on the urea increase the reaction rate).

Finally, the most interesting result in this latter batch is the observation that methylation of the nitrogen atom in **5** results in a much less efficient addition. Given that the oxo groups next to the vanadium atoms have a higher negative charge density they might develop a H-bond[31–34] with the incoming indole nucleophile, resulting in a kind of pre-arrangement favoring the addition. This secondary interaction would disappear upon methylation of the indole.

One of the main features of the organo-POM catalysts is that they can be easily recycled upon precipitation.[35,36] Therefore the catalytic reaction with **1a** was carried out in a centrifugation tube. At the end of the reaction the catalyst was precipitated with in diethyl ether, the reaction mixture was then centrifuged at 5000 rpm. The organic phase was filtered off and the centrifugation tube reloaded with a new batch of reagents. The process was repeated three times. In all cases, the conversion profiles of the reaction were very similar, showing that in that case also the POM framework enabled simplified recycling of the catalytic system.

Finally, we prepared the POM dimer 6 from the corresponding bis-urea (Scheme 1). **6** was obtained in 75% yield. The yield obtained was slightly lower compared to the single POMs. It may be due to the higher charge of the POM. However, **6** is very pure with no observable sign of mono-grafted POM.

Figure 2. Reactions of different indoles. POM 1c was used as catalyst (2 mol%).

Scheme 1. Synthesis of bis-urea organo-POM **6**.

POM **6** was selected to examine possible cooperative effects. Hence the flexible hexamethylene spacer. **6** was engaged in the catalytic reaction. In that case, only 1 mol% of it was used, to keep the same overall amount of catalytic sites. The conversion reached 56% after four days, where the corresponding equivalent single-site 1e stopped at 48% (at 2 mol% loading). This suggests that there may be some cooperativity that improved the overall efficiency.

In conclusion, a new class of catalytic reactions – H-bond organocatalysis – has been opened to organo-POMs. The unique interplay between a urea function embedded into a POM framework has been studied with the help of modeling. It enabled the catalysis of the Friedel-Crafts alkylation of indoles with *trans*-β-nitrostyrene, and the catalyst could be recycled several times. The highly electron-withdrawing polyoxometalate scaffold likely augments the ureic protons acidity, which accelerates the Friedel-Crafts alkylation relative to the free urea ligands. We believe that the POM structure also participates. Some of the oxo ligands in the trivanadium crown are highly polarized and likely to help the catalytic activity by developing H-bonds to the nucleophile, thus pre-arranging the reagents. Finally, there seems to be cooperativity in dual-site compounds. Further work will focus on fully probing these two latter issues, as well as use our modeling to build a chiral pocket around the catalytic site.

[1] D. Ravelli, S. Protti, M. Fagnoni, *Acc. Chem. Res.* **2016**, *49*, 2232–2242.
[2] I. A. Weinstock, R. E. Schreiber, R. Neumann, *Chem. Rev.* **2018**, *118*, 2680–2717.
[3] M. Samaniyan, M. Mirzaei, R. Khajavian, H. Eshtiagh-Hosseini, C. Streb, *ACS Catal.* **2019**, *9*, 10174–10191.
[4] M. Stuckart, K. Yu. Monakhov, *Chem. Sci.* **2019**, *10*, 4364–4376.
[5] N. Li, J. Liu, B.-X. Dong, Y.-Q. Lan, *Angew. Chem. Int. Ed.* **2020**, *59*, 20779–20793.
[6] J. Jiang, O. M. Yaghi, *Chem. Rev.* **2015**, *115*, 6966–6997.
[7] M. J. Da Silva, N. A. Liberto, *Curr. Org. Chem.* **2016**, *20*, 1263–1283.
[8] F. Lefebvre, *Curr. Catal.* **2017**, *6*, 77–89.
[9] M. Jose da Silva, C. Macedo de Oliveira, *Curr. Catal.* **2018**, *7*, 26–34.
[10] S. Luo, J. Li, H. Xu, L. Zhang, J.-P. Cheng, *Org. Lett.* **2007**, *9*, 3675–3678.
[11] G. Raj, C. Swalus, A. Guillet, M. Devillers, B. Nysten, E. M. Gaigneaux, *Langmuir* **2013**, *29*, 4388–4395.
[12] A. Misra, K. Kozma, C. Streb, M. Nyman, *Angew. Chem. Int. Ed.* **2020**, *59*, 596–612.
[13] A. Dolbecq, E. Dumas, C. R. Mayer, P. Mialane, *Chem. Rev.* **2010**, *110*, 6009–6048.
[14] A. J. Kibler, G. N. Newton, *Polyhedron* **2018**, *154*, 1–20.
[15] Q. Xu, X. Liang, B. Xu, J. Wang, P. He, P. Ma, J. Feng, J. Wang, J. Niu, *Chem. Eur. J.* **2020**, *26*, 14896–14902.
[16] L. Lian, X. Chen, X. Yi, Y. Liu, W. Chen, A. Zheng, H. N. Miras, Y.-F. Song, *Chem. Eur. J.* **2020**, *26*, 11900–11908.
[17] Y. Benseghir, A. Lemarchand, M. Duguet, P. Mialane, M. Gomez-Mingot, C. Roch-Marchal, T. Pino, M.-H. Ha-Thi, M. Haouas, M. Fontecave, A. Dolbecq, C. Sassoye, C. Mellot-Draznieks, *J. Am. Chem. Soc.* **2020**, *142*, 9428–9438.
[18] H. Omachi, T. Inoue, S. Hatao, H. Shinohara, A. Criado, H. Yoshikawa, Z. Syrgiannis, M. Prato, *Angew. Chem. Int. Ed.* **2020**, *59*, 7836–7841.
[19] A. Blanc, P. de Fremont, *Chem. Eur. J.* **2019**, *25*, 9553–9567.
[20] M. Attoui, E. Pouget, R. Oda, D. Talaga, G. Le Bourdon, T. Buffeteau, S. Nlate, *Chem. Eur. J.* **2018**, *24*, 11344–11353.
[21] J. Li, I. Huth, L.-M. Chamoreau, B. Hasenknopf, E. Lacôte, S. Thorimbert, M. Malacria, *Angew. Chem. Int. Ed.* **2009**, *48*, 2035–2038.
[22] J. Oble, B. Riflade, A. Noël, M. Malacria, S. Thorimbert, B. Hasenknopf, E. Lacôte, *Org. Lett.* **2011**, *13*, 5990–5993.
[23] B. Riflade, D. Lachkar, J. Oble, J. Li, S. Thorimbert, B. Hasenknopf, E. Lacôte, *Org. Lett.* **2014**, *16*, 3860–3863.
[24] I. Azcarate, Z. Huo, R. Farha, M. Goldmann, H. Xu, B. Hasenknopf, E. Lacôte, L. Ruhlmann, *Chem. Eur. J.* **2015**, *21*, 8271–8280.
[25] D. Lachkar, D. Vilona, E. Dumont, M. Lelli, E. Lacôte, *Angew. Chem. Int. Ed.* **2016**, *55*, 5961–5965.
[26] W.-K. Miao, Y.-K. Yan, X.-L. Wang, Y. Xiao, L.-J. Ren, P. Zheng, C.-H. Wang, L.-X. Ren, W. Wang, *ACS Macro Lett.* **2014**, *3*, 211–215.
[27] K. Hof, M. Lippert, P. R. Schreiner, Georg Thieme Verlag, **2012**, p. 297.
[28] A. G. Doyle, E. N. Jacobsen, *Chem. Rev.* **2007**, *107*, 5713–5743.
[29] M. J. Frisch, et al., *Gaussian 16 Rev. C.01*, Wallingford, CT, **2016**.
[30] R. P. Herrera, V. Sgarzani, L. Bernardi, A. Ricci, *Angew. Chem. Int. Ed.* **2005**, *44*, 6576–6579.
[31] C. Boglio, K. Micoine, É. Derat, R. Thouvenot, B. Hasenknopf, S. Thorimbert, E. Lacôte, M. Malacria, *J. Am. Chem. Soc.* **2008**, *130*, 4553–4561.
[32] D. Vilona, D. Lachkar, E. Dumont, M. Lelli, E. Lacôte, *Chem. Eur. J.* **2017**, *23*, 13323–13327.
[33] Z.-M. Zhang, X. Duan, S. Yao, Z. Wang, Z. Lin, Y.-G. Li, L.-S. Long, E.-B. Wang, W. Lin, *Chem. Sci.* **2016**, *7*, 4220–4229.
[34] T. Noguchi, C. Chikara, K. Kuroiwa, K. Kaneko, N. Kimizuka, *Chem. Commun.* **2011**, *47*, 6455–6457.
[35] N. Dupré, P. Rémy, K. Micoine, C. Boglio, S. Thorimbert, E. Lacôte, B. Hasenknopf, M. Malacria, *Chem. Eur. J.* **2010**, *16*, 7256–7264.
[36] C. Boglio, G. Lemière, B. Hasenknopf, S. Thorimbert, E. Lacôte, M. Malacria, *Angew. Chem. Int. Ed.* **2006**, *45*, 3324–3327.
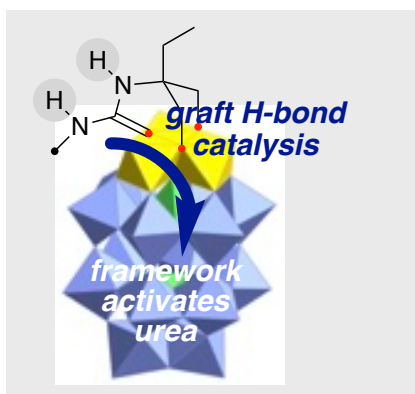
Entry for the Table of Contents (Please choose one layout)

Layout 1:

COMMUNICATION

Hydrogen-bond catalysis is implanted into polyoxometalates (POMs) via the insertion of ureas into the framework. A likely combination of electron-withdrawing effects and double activation via the metal-oxo surface enables urea catalysis in POMs. The organopolyoxometalate catalysts can be recycled and reused several times. Modeling and NMR are used to investigate this new POM property.

Debora Vilona, Moreno Lelli,* Elise Dumont,* Emmanuel Lacôte*

Page No. – Page No.

Organo-polyoxometalate-Based Hydrogen-Bond Catalysis